Experimental verification of the stochastic model for predicting the performance of Oscillating Water Colums devices

Sergio M Camporeale[1] and Pasquale G. F. Filianoti[2]

[1] "Politecnico di Bari" University –DIMEG Department
E-mail: camporeale@poliba.it
[2] University Mediterranean of Reggio Calabria – Okeanòs Laboratory
e-mail: filianoti@unirc.it

Abstract

Stochastic models are often used to evaluate the average power output of an oscillating-water-column (OWC) wave power plant equipped with a Wells turbine and for defining optimal control criteria of the system. The application of the stochastic model to OWC devices is based on the hypothesis that the dynamic behavior of the system can be modeled by a set of linear differential equations and that the sea surface elevation, acting as an input, has a Gaussian probability density function. Under such hypotheses, from the theory of the random processes of the linear systems, it comes that the outputs of the system, such as the pressure in the chamber and the turbine flow coefficient, have a gaussian distribution. Actually, there are several non-linear phenomena that can alter the linear behavior of a OWC device:

- minor and major losses of the unsteady flow of water and air;
- compressibility of air and heat exchange with the walls of the air chamber;
- non-linear characteristics of the turbine.

The stochastic model can be applied if such non-linearities have, on the whole, limited effects or if a specific procedure able to take them into account is adopted, as suggested by the authors in previous papers.

In the Authors' knowledge, no experimental validation of the application of the stochastic model to OWC devices are present in the open literature.

This work, making use of data gathered during the experiment on a 1:10 scale model of a ocean OWC breakwater, put at the sea off the beach of Reggio Calabria, aims at verifying that the energy conversion process inside the OWC can be actually described as a gaussian process. To this purpouse, the frequency distribution of the main physical parameters, relevant to the system dynamics, are evaluated. Moreover, in order to characterize the behavior of the Wells turbine, the experimental values of the time averaged turbine torque and pressure drop are evaluated as a function of the variance of the flow coefficient. The results show a very high level of correlation and a very good agreement with those that can be obtained from the application of the stochastic model, using as an input the characteristic curves of the turbine, yelded in the unsteady flow.

Keywords: breakwater converter, stochastic approach, linearized model, Wells turbine, random waves.

Nomenclature

A	= absorption coefficient, section area
A_t	= turbine bladed area
B_t	= turbine Damping Factor
c	= height of the room containing the water column
C_L	= adequacy coefficient
d	= water depth
D	= air tube and turbine, diameter
$\mathscr{E}$	= wave energy per unit surface
f	= friction factor
F_t	= applied turbine damping factor
g	= gravitation acceleration
G	= coefficient of differential equation
h	= hub-to-tip ratio, energy per unit weight
H	= wave height, total hydraulic head
k	= wave number
l	= duct length
m	= air polytropic law exponent
m_0	= zeroth order moment of the spectrum
p	= pressure
p_G	= Gaussian probability density function
P_a	= plant absorbed power
P_p	= turbine available power
P_t	= turbine shaft power
Q	= flow rate
$\mathscr{R}$	= hydraulic radius
s	= width of the vertical duct, blade solidity
s'	= width of the OWC
t	= time
T	= wave period
u	= flow velocity
U_{tip}	= tangential tip velocity
Y	= head losses
z	= vertical coordinate axis with origin at the mean water level (m.w.l.)
β	= amplification factor
δ	= phase angle

Δp = pressure drop
φ = turbine flow coefficient
λ = friction factor
η_t = turbine efficiency
ρ = mass density [kg/m^3]
σ = standard deviation
Φ = wave energy flux
ψ^* =. narrow bandedness parameter
ω = angular frequency [rad/s]
ζ = height of the air pocket

Superscripts

— = Overbar for time average quantity
$*$ = dimensionless value

Subscripts

0 = still water condition
a = air
A = OWC horizontal section at air-water interface
B = vertical duct hotizontal section at the outer opening
c = continuous
i/s = minor head losses
l = loss
p = relevant to the peak frequency of the spectrum
s = significant
w = water
t = turbine

1 Introduction

A realistic performance analysis of OWC wave energy converters addresses to a set of non-linear differential equations that need to be integrated in time, by using a stochastic approach, under the hypothesis of random wind-generated sea waves, for all the sea states which characterize the location of the system. Non-linearities of the differential equations have several origins:

i) minor and major losses of the unsteady flow of water and air;

ii) compressibility of air and heat exchange with the walls of the air chamber;

iii) non-linear characteristics of the turbine.

A time-domain analysis [1], [2] allows to deal more realistically with non-linear power take-off equipment; yielding the performance variables (namely power output) as functions of time [3]. Time series for variables like rotational speed and electrical power output are important to study, for example, power oscillations induced by wave grouping or to develop plant control strategies. However, predictions of average power output in a given sea state may be sufficient for most purposes in plant design [4], including the specification of the power equipment (turbine and generator). These predictions may be provided by stochastic methods that are computationally much less demanding, as it has been shown in [4].

Here, we propose an original methodology for linearizing the differential equations that describe the system behaviour. The model is based on hypotheses of random sea waves with small amplitudes (representing a gaussian process of time) and linear turbine characteristic. The developed methodology has been applied for estimating the performance of the new OWCs family, called REWEC, patented by Boccotti in 1998, and consisting of several caissons, embodying an OWC with additional vertical duct. The structure is similar to caissons of traditional breakwaters, that placed on the seabed, close one to each other, form a breakwater-converter. Each caisson is connected to the sea by a vertical duct wholly beneath the sea level, and to the atmosphere by an air duct where a Wells turbine is placed.

The interaction between the waves and the plant is presented in Section 2. In Section 3, the non-linear differential equations describing the flow inside the plant are linearized. In particular, it is shown that the motion of water and air through the plant can be assimilated to the motion of a linear mechanical system constituted by masses springs and viscous dampers.

The application of the methodology is illustrated by numerical examples in Section 4, assuming a proportionality relationship (at constant rotational speed) between turbine flow rate and pressure drop. Average values for the power output and efficiency can then be easily obtained from the turbine instantaneous performance curves, got under unsteady flow conditions, and the pressure probability density function.

2 OWC plant − sea waves interaction

2.1 The wave motion at the OWC wall

The problem of the wave motion before the breakwater has been solved in [5], on supposing that there may be whichever periodic waveform with the given frequency and a mean energy flux smaller than (or equal to) the mean energy flux of the incident waves. Then, looking for the waveform which satisfies the equations of wave-OWC interaction, and gives the largest value of $\overline{\Phi}/\overline{\mathscr{E}}$ (=mean energy flux / mean energy per unit surface), it has been shown that, in some cases the wave motion before the breakwater is the superimposition of the standing waves, yielded by the reflection of the incident waves, with a progressive wave generated by the water discharge through the plant (solution S_1). In other cases the solution giving the largest value of $\overline{\Phi}/\overline{\mathscr{E}}$ proves to be a sum of two standing waves with phase angles in space and time (solution S_0). In these cases (sum of two standing waves) the plant may absorb up to the 100% of the incident wave energy.

The solution S_1 takes place when the absorber and waves are close to resonance. Resorting to the resonance coefficient R [5], we are able to asses the plant operating conditions. With $R = 0$ the plant works in a resonance condition, in that the time lag between wave pressure $\Delta p(t)$ on the outer opening of the vertical duct and the water discharge Q_p through the plant (positive if the water enters the plant) is equal to zero. R greater than zero means that the eigenperiod of the plant is greater than the wave period. On the contrary, R smaller than zero means that the eigenperiod of the plant is smaller than the wave period.

The experimental results [6] on a small scale model of REWEC, placed directly at sea, reveal that solution S_1 (superimposition of standing with progressive waves) works rather well for wind-waves, and leads to a reduction of the wave height at the breakwater-converter in respect of the wave height at a conventional reflecting breakwater. While the solution S_0 (superimposition of two standing waves) happens with some swells, and it leads to an amplification of the wave height at the breakwater-converter, in respect of the wave height at a conventional reflecting breakwater (i.e. the wave height at the converter is greater than two times the incident wave height). Commonly, for many swells the actual situation proved to be between solution S_1 and S_0. From solution S_1 to solution S_0 the wave height at the breakwater converter grows the more the greater the $|R|$ is. As a consequence, also the energy absorbed by the plant is increased. However the largest absorption coefficients (=absorbed energy / incident energy) continue to occur with small $|R|$, that is with the plant working close to the resonance condition.

The $\Delta p(t)$ acting on the outer opening of the vertical duct must be given as an input in the model. Hereafter, for checking the linearization procedure, we used the time series of $\Delta p(t)$ actually recorded on the physical model put at sea. Alternatively, for design purposes, the $\Delta p(t)$ can be numerically simulated using the form

$$\Delta p(t) = \beta\rho g \sum_{i=1}^{N} H_i \frac{\cosh[k_i(d+z_o)]}{\cosh(k_i d)} \cos(\omega_i t + \delta_i)\,, \quad (1)$$

where β is the amplification factor (= the quotient between the r.m.s. wave height at the breakwater converter and the r.m.s. wave height at a conventional reflecting breakwater). Eq. (1) represents pressure fluctuations in a sea state given that: H_i and ω_i are such as to form a characteristic spectrum of sea waves, and k_i is related to ω_i by the linear dispersion rule; phase angles δ_i are distributed uniformly in $(0,2\pi)$ and are stochastically independent of one another; moreover the number N must be very large.

In [5] the value of β is chosen among the ∞^1 solutions which fulfill, at every time instant, the conditions that:

(i) the water discharge entering (or exiting from) the plant must be equal to the water discharge of the wave at the converter;

(ii) the energy flux absorbed by the plant must be equal to the wave energy flux at the breakwater-converter.

The selected β is the one giving the largest value of the quotient between mean energy flux $\overline{\Phi}$, and mean energy per unit surface $\overline{\mathscr{E}}$ (i.e. the largest value of the propagation speed of the wave energy reflected towards the open sea by the breakwater-converter).

We will adopt a simpler procedure for the calculation of β, based on an heuristic approach [7]. As a first step, we shall fix a trial value β_1, so as to obtain $\Delta p(t)$ from eq. (1), wherein amplitudes H_i and frequencies ω_i are obtained discretizing the JONSWAP spectrum (see § 2.2 for details), and phases δ_i are generated randomly. So doing, the generated $\Delta p(t)$ is a stationary random process with a Gaussian distribution [8]. Then, solving the equations explained in Sect. 2.2 for the flow inside the plant, we calculate the ratio A_1, between the energy absorbed by the plant and the energy of the incident waves. The new trial value β_2 follows from

$$\beta_{i+1} = 1 - A_i\,. \quad (2)$$

A few iterations suffice to achieve the convergence.

Differences between this approach and the physical approach developed in [5] for the calculation of β have no consequences in the design process, neither in terms of structural stability of the breakwater, nor in terms of performance optimization of the converter. In fact, the breakwater overall stability must be assessed under the action of extreme wave groups where, in order to achieving a safety advantage, any reduction of wave height due to energy absorption by the plant is neglected (i.e. the plant is deactivated). While the optimal design of the converter (that is the design able to maximize the annual energy production) is achieved tuning the plant to work close to the resonance condition ($R \cong 0 \;\rightarrow$ solution S_1), with the waves conveying the most energy on annual basis.

Differences only affect the estimation of energy production. For wind-waves the results obtained with the above explained procedure are quite similar to those obtained with the theory, while for the swells they underestimate the energy absorbed by the plant [8].

2.2 The water/air motion inside the plant

There are two embodiments of the plant, depending on the cells of a caisson are interconnected among them or not. In the plant with independent cells (see Fig. 1), each caisson of the breakwater consists typically of three independent cells, each with its own air tube (embodiment OWC/3). In the plant with interconnected cells there are some holes which let air flow from one cell to the adjacent ones of the same caisson (embodiment OWC/1), and there is one air tube connecting the cells to the atmosphere (see Fig. 2).

The flow equation of the water inside one cell (not connected with other cells) may be written in the form

$$\frac{c-\zeta}{g}\frac{\mathrm{d}^2\zeta}{\mathrm{d}t^2} + \frac{l}{g}\frac{\mathrm{d}u_\mathrm{w}}{\mathrm{d}t} = H_A - H_B - \sum Y, \quad (3)$$

where l is the length of the vertical duct, ζ is the height of the air pocket, c is the height of the inner room, u_w is the velocity in the vertical duct (positive upward). The total head H_A is related to the (absolute) pressure p_a in the air pocket:

$$H_A = \zeta_0 - \zeta + \frac{p_a - p_{a0}}{\rho_w g} + \frac{(\mathrm{d}\zeta/\mathrm{d}t)^2}{2g}, \qquad (4)$$

where ζ_0 is the still water value of ζ. The total head H_B is related to the wave pressure Δp at the outer opening of the vertical duct:

$$H_B = \Delta p_B / \rho_w g \,. \qquad (5)$$

Head losses, both continuous (Y_c) and minor ($Y_{i/s}$), can be expressed in the form valid for permanent flows:

$$\sum Y = Y_c + Y_{i/s} = \frac{1}{2g}\left(\frac{\lambda_w}{4\mathcal{R}} l + K_w\right)|u_w|\, u_w\,, \qquad (6)$$

where $\mathcal{R}$ is the hydraulic radius, λ_w is the friction factor, and K_w is the loss coefficient, assumed as unique value independently from the flow direction.

The flow velocity in the vertical duct u_w, is related to the time derivative of ζ by the continuity equation:

$$u_w = \frac{s'}{s}\frac{d\zeta}{dt}\,, \qquad (7)$$

where s is the width of the vertical duct and s' is the width of the oscillating water column.

Expanding terms H_A, H_B, ΣY, and u_w, in Eq. (3), by means of eq. (4), (5), (6), and (7), respectively, we obtain

$$G\frac{\mathrm{d}^2 y_1}{\mathrm{d}t^2} - \frac{B_w}{g}\left|\frac{\mathrm{d}y_1}{\mathrm{d}t}\right|\frac{\mathrm{d}y_1}{\mathrm{d}t} + \frac{p_a - p_{a0}}{\rho_w g} + y_1 = \Delta p_B(t)\,, \qquad (8)$$

where $$G \equiv \frac{1}{g}\left(\frac{ls'}{s} + c - \zeta\right), \qquad (9a)$$

and $$B_w \equiv \frac{1}{2}\left(\frac{\lambda_w}{4\mathcal{R}} l + k_w\right)\left(\frac{s'}{s}\right)^2, \qquad (9b)$$

and $y_1 (= \zeta - \zeta_0)$ is the displacement of the water surface in the air chamber.

Assuming that the pressure p_a inside the chamber varies according to the polytrophic law

$$\frac{p_a}{p_{a0}} = \left(\frac{\rho_a}{\rho_{a0}}\right)^m, \qquad (10)$$

the velocity in the air tube is related to pressure p_a by the relation

$$l_a \frac{\mathrm{d}u_a}{\mathrm{d}t} = \frac{p_a}{\rho_{a0}}\frac{m}{m-1}\left[\left(\frac{p_a}{p_{a0}}\right)^{1-1/m} - 1\right] - g\Delta h_a\,, \qquad (11)$$

where

$$\Delta h_a = \frac{1}{2g}\left(\frac{\lambda_a}{D} l_a + K_a\right)|u_a|\, u_a + \frac{F_t}{g} u_a\,, \qquad (12)$$

accounts for the energy dissipation (per unit weight) in the air tube due to continuous (friction factor: λ_a) and minor (loss coefficient: K_a) losses, and due to the pressure drop across the turbine (applied turbine damping factor: F_t).

Considering operating conditions into which the turbine damping factor B_t is almost constant, F_t can be determined from the geometrical characteristics and the rotational speed of the turbine:

$$F_t = \frac{B_t U_{tip}}{2}\frac{A_a}{A_t}\,. \qquad (13)$$

where U_{tip} is the tangential velocity at the blade tip, and A_t is the turbine bladed area.

Expanding terms Δh_a, and F_t in equations (11) and (12), respectively by means of equations (12) and (13), we obtain

$$l_a \frac{\mathrm{d}u_a}{\mathrm{d}t} + B_a|u_a|u_a - \frac{p_{a0}}{\rho_a}\frac{m}{m-1}\left[\left(\frac{p_a}{p_{a0}}\right)^{1-1/m} - 1\right] + F_t u_a = 0 \qquad (14)$$

where

$$B_a \equiv \frac{1}{2}\left(\frac{\lambda_a}{D} l_a + k_a\right), \qquad (15)$$

The rate of change of the air mass M_a in the air pocket is related to u_a and ρ_a:

$$\frac{\mathrm{d}M_a}{\mathrm{d}t} = -\rho_a \frac{\pi D^2}{4} u_a\,. \qquad (16)$$

Equations (8) and (14) can be solved numerically for given $H_B(t)$ and initial conditions.

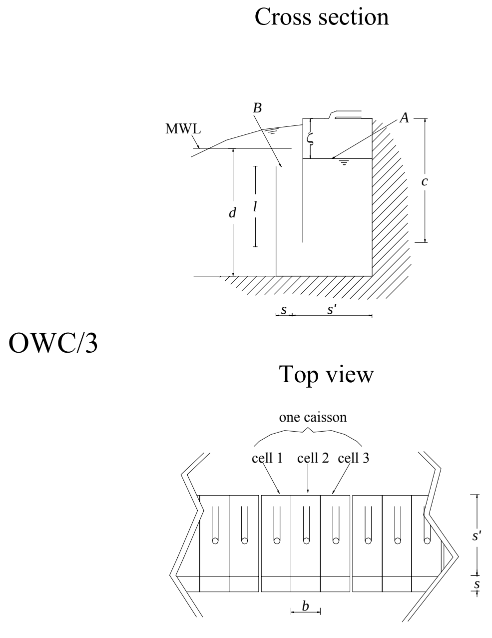

Fig. 1: Reference scheme OWC/3

With the cells interconnected among them (OWC/1), we have three elevations ζ_1, ζ_2, ζ_3, three air masses

M_{a1}, M_{a2}, M_{a3}, three air pressures p_{a1}, p_{a2}, p_{a3}, three air velocities u_{a1}, u_{a2}, u_{a3}, all generally different from one another.

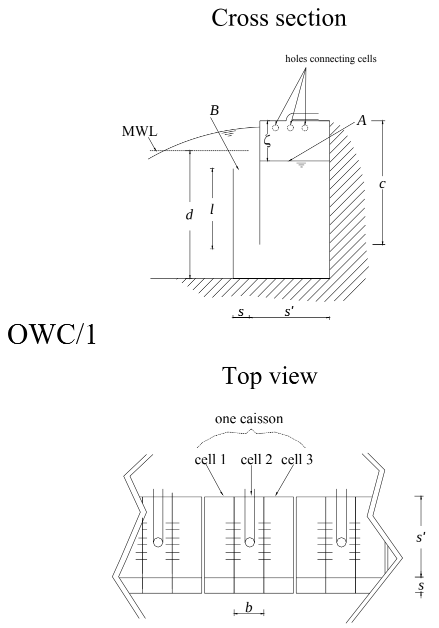

Fig. 2: Reference scheme OWC/1.

Here u_{a1} and u_{a2} are the air velocities, respectively, in the holes connecting cell 1 with cell 2 (the central one), and in the holes connecting cell 3 with cell 2. The equations of the air velocity for cells 1 and 3 become respectively

$$\widetilde{K}_a \frac{u_{ai}^2}{2}\frac{u_{ai}}{|u_{a1}|} = \frac{p_{a0}}{\rho_{a0}}\frac{m}{m-1}\left[\left(\frac{p_{ai}}{p_{a0}}\right)^{1-1/m} - \left(\frac{p_{ai}}{p_{a0}}\right)^{1-1/m}\right] \quad i = 1,..3 \quad (17)$$

where $\widetilde{K}_a$ is the coefficient of losses in the holes connecting two adjacent cells. Moreover, the equations of the rate of change of the air mass become

$$\frac{\mathrm{d}M_{ai}}{\mathrm{d}t} = -\rho_a A_H u_{ai}, \quad i = 1,3, \qquad (18a)$$

$$\frac{\mathrm{d}M_{a2}}{\mathrm{d}t} = -\left(\frac{\mathrm{d}M_{a1}}{\mathrm{d}t} + \frac{\mathrm{d}M_{a3}}{\mathrm{d}t}\right) - \rho_a \frac{\pi D^2}{4} u_{a2}, \quad (18b)$$

where A_H is the section area of the holes connecting two adjacent cells.

The mathematical model given by Equations (8), (14) and (16) has been validated and calibrated against the experimental results obtained in the field on a small scale model without turbine [6]. Details on the calibration of the exponent m of the polytrophic law and coefficients λ_a, $K_{i/s}$, $\widetilde{K}_a$ of the minor losses can be found therein.

3 The linearized model

3.1 Outline of the procedure

Design and performance estimation have been carried out by using a linearized form of Equations (8), (14) and (16), obtained considering small displacement of ζ from the value of static equilibrium ζ_0, and an incompressible flow in the air tube. The linearized form consists of a couple of 2nd order ordinary differential equations, analogous to the equations that describe the mechanical spring-mass-damper system shown in Fig. 3.

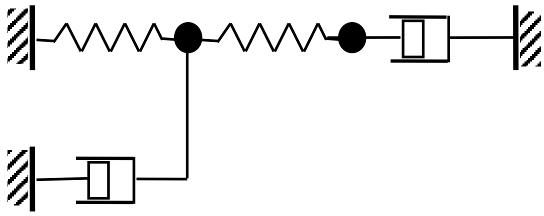

Fig. 3: The mechanical system equivalent to REWECs.

The terms that need to be linarised are:

(i) the characteristic curve [$\Delta p^* = f(\varphi)$] of the Wells turbine;
(ii) the polytrophic law of air in the air pocked (acting as a gas spring);
(iii) the hydraulic losses both minor and major.

Linearization of term G in Eq. 8 follows straightforwardly by the Taylor series polynomial of degree 1:

$$G = \left(\frac{ls'}{s} + c - \zeta_0\right). \qquad (18)$$

Calculation of p_a follows from the Taylor series polynomial of degree 1 of Eq. (10) and the continuity equation (15):

$$p_a = p_{a0}\left[1 - \frac{m}{\zeta_0}\left(y_1 + \frac{A_a}{bs'}y_2\right)\right], \qquad (19)$$

where y_2 is the particle displacement in the air tube ($u_a = \mathrm{d}y_2 / \mathrm{d}t$).

3.2 Linearization of energy losses

In order to describe the procedure adopted to linearize head losses both in the water and in the air flow, we suppose first that the wave acting on the system is a simple sinusoidal wave. Under such hypothesis, the integration of the non-linear differential equations (8) and (14), leads to a periodic solutions $y_1(t)$, $y_2(t)$ that are not far from sinusoidal functions of time. Assuming for $y_1(t)$, $y_2(t)$ a sinusoidal form with period T, power losses due to continuous and minor losses in the vertical duct and in the air tube can be evaluated as

$$\overline{P_l} = \frac{\rho g A}{T} K_l \int_t^{t+T} |u| u^2 \, dt \, , \tag{20}$$

where coeffcient K_l accounts for all the considered turbulent losses in the flow (either water flow or air flow).

In the linear model, head losses vary linearly with the flow velocity (u_w in the vertical duct, u_a in the air tube), like in a laminar flow. In such conditions power losses should be equal to those of the non-linear system with the same period T and the same velocity u :

$$\overline{P} = \frac{\rho g A}{T} K_{l\,eq} \int_t^{t+T} u^2 \, dt \, . \tag{21}$$

Under the above hypotheses on $y_1(t)$ and $y_2(t)$, also $u_w(t)$ and $u_a(t)$ are sinusoidal functions with amplitudes u_{ow} and u_{oa}, respectively. Equating the r.h.s. of Eqs. (20) and (21), it is straightforward to obtain the equivalent head losses coefficient

$$K_{l\,eq} = K_l \frac{8 u_o}{3\pi} \, . \tag{22}$$

Then, it is possible to rewrite Eqs. (8) and (14) in the linearised form, replacing terms $|u_w| \, (= |\mathrm{d}y_1/\mathrm{d}t|)$ and $|u_a| \, (= |\mathrm{d}y_2/\mathrm{d}t|)$ with adequacy coefficients C_{lw} and C_{la} (= turbulent flow mean energy losses / laminar flow mean energy losses) respectively equals to $8u_{ow}/(3\pi)$ and $8u_{oa}/(3\pi)$. C_{lw} and C_{la} can be determined by means of an iterative procedure: starting with a tentative value of amplitudes u_{ow}, u_{oa}, the linearized differential equations can be integrated and new values can be obtained for u_{ow}, u_{oa}. The iterations can be carried out until the convergence values are obtained.

Considering the more realistic case of a breakwater-converter interacting with irregular sea waves, mean adequacy coefficients $\overline{C}_{lw}, \overline{C}_{la}$ can be obtained as follows.

Assuming that the randomly oscillating flows inside the vertical duct and the air tube are stationary Gaussian processes with an infinitely narrow spectrum, the $\overline{C}_l$ for a sequence of wind waves (sea state) is given by

$$\overline{C}_l = \int_0^\infty C_l \, p_G(u; \sigma_u = w) \mathrm{d}u \, , \tag{23}$$

where the product $p_G(u; \sigma_u = w)\mathrm{d}u$ is the probability of a velocity amplitude within the fixed small interval [u, u+ du], in a sea state with a given standard deviation σ_u equal to w. The probability density assumes the form

$$p_G(u; \sigma_u = w) = \frac{u}{\sigma_u^2} \exp\left(-\frac{u^2}{2\sigma_u^2} \right) \tag{24}$$

which substituted in Eq. (23) permits to solve the integral, bringing to

$$\overline{C}_L = \frac{4}{3} \sqrt{\frac{2}{\pi}} \sigma_u \, . \tag{25}$$

Some kinematic and dynamic properties of characteristic sea wave groups occurring during sea states, like particle velocity and acceleration, may be effectively represented using the simple functions valid for periodic waves, assuming $H = H_s$ and $T = T_p$. Also the shoaling-refraction of the wind waves may be effectively estimated in the same manner [6]. So, we can retain that the dynamic behaviour of the plant under the action of irregular sea waves is characterized by a core of waves "significant" acting on the outer opening of the vertical duct. We can identify these significant waves as the third part of highest waves occurring during the sea state. Consequently, calculating the average C_l of the 1/3 highest waves of the velocity fluctuations inside the vertical duct (or the air tube), it is possible to show that

$$\overline{C}_{l_{1/3}} = \frac{\int_{U_{1/3}}^\infty C_l \, p_G(u; \sigma_u = w) \mathrm{d}u}{\int_{U_{1/3}}^\infty p_G(u; \sigma_u = w) \mathrm{d}u} \, , \tag{26}$$

where $U_{1/3}$ is the threshold being exceeded by 1/3 wave heights of velocity fluctuations. This definition is simply expressed by

$$U_{1/3} = \sigma_u \sqrt{8 \ln 3} \, . \tag{27}$$

Solving the integrals in Eq. (26), we arrive to

$$\overline{C}_{l_{1/3}} = \frac{16}{3\pi} \sigma_u \, . \tag{28}$$

Also in this case an iterative procedure is necessary to evaluate σ_{uw}, σ_{aw}; in all the tested cases, a few iterations have been needed to reach convergence.

3.3 Estimation of the power output

A stochastic approach has been used in order to estimate the power output [4]. The total head $H_B(t)$ (Eq. 5) acting on the outer opening of the vertical duct can be evaluated by using the expression (1) for the pressure fluctuations $\Delta p_B(t)$ and the procedure explained in Sect. 2.1 for the calculation of the amplification factor β.

The power absorbed by the plant is given by the product of the instantaneous water flow rate Q_w through the vertical duct and the pressure fluctuations $\Delta p_B(t)$:

$$P_a(t) = Q_w \Delta p_B = b s u_w(t) \Delta p_B(t) \, . \tag{29}$$

The power P_p absorbed by the turbine is given by the product of the instantaneous air flow rate Q_a through the air tube and the pressure drop $\Delta p_t(t)$ across the turbine:

$$P_p(t) = \Delta p_t Q_a = \frac{1}{2} \rho_a \Delta p_t^* U_{tip}^2 A_t u_a(t) \, , \tag{30}$$

where Δp_t^* is the non-dimensional pressure drop:

$$\Delta p_t^* = B_t u_a / U_{tip} = B_t \varphi \, . \tag{31}$$

The power output P_t follows straight from the product of P_p with the turbine efficiency $\eta_t(\varphi)$ (got under unsteady flow conditions):

$$P_t = \frac{1}{2}\rho_a\, U_{tip}^3 A_t B_t \varphi^2 \eta_t\,. \qquad (32)$$

Being $H_B(t)$ a gaussian process, also $y_1(t)$ and $y_2(t)$ are gaussian processes of time in the linearized model, thereafter also $\varphi(t)$ is Gaussian, consequently the average power output is given by

$$\overline{P}_t = \frac{1}{2}\rho_a\, U_{tip}^3 A_t B_t \int_0^{+\infty} \eta_t(\varphi)\varphi^2 p_G(\varphi;\sigma_\varphi = w)\mathrm{d}\varphi\,, \qquad (33)$$

where, and $\sigma_\varphi \equiv \sigma_{u_a}/U_{tip}$ is the standard deviation of the non-dimensional flow coefficient φ.

Finally, the average turbine efficiency $\overline{\eta}_t$ can be expressed in the form

$$\overline{\eta}_t = \frac{\overline{P}_t}{\overline{P}_p} = \frac{\int_0^{+\infty} \eta_t(\varphi)\varphi^2 p_G(\varphi;\sigma_\varphi = w)\mathrm{d}\varphi}{\sigma_\varphi^2}\,. \qquad (34)$$

4 Results

4.1 Model validation vs experimental data

To validate the linearization procedure, the OWC/1 running has been simulated by numerically integrating in the time domain equations (8), (14) and (15), linearized through the procedure outlined above. As for pressure fluctuations acting on the outer opening of the vertical duct (Eq. 1), the actual time series recorded at sea on the physical model [5] has been used.

Performance data $\Delta p_t^*, \eta_t$ vs φ (Fig. 4) obtained as a regression of experimental data have been used in the model too.

Fig. 5 shows a 100 s time frame of the pressure fluctuations Δp measured (red line) into the central cell of the breakwater middle caisson, during a sea state with H_s = 0.43 m of significant wave height. Narrow bandedness parameter ψ^* = 0.76 reveals that waves are wind generated [6]. The peak period T_p of the power spectrum is equal to 2.8 s. the turbine rotational speed is 1600 rpm. The green line has been obtained with the linear model. Figs 6 – 8 show, for the same record and time span, comparisons between water discharge, pneumatic power and internal turbine power, respectively.

As we can see, the agreement between experimental and numerical data is rather accurate. Some minor differences are due to the use of regressive curves of Fig. 4. These differences become more evident during the occurrence of highest sea waves groups, because of non-linearity effects growing. Tab. 1 shows the r.m.s. values of Δp and Q, and the mean pneumatic and internal turbine power, relevant to the entire duration of record N. 20 (i.e. 300 s). The model tends to overestimate the amplitude of the pressure fluctuations by 30%. Conversely, it underestimate the water discharge by about 10%. Therefore, a better tuning can be achieved on fine adjusting the loss coefficients λ_a, $K_{i/s}$, $\widetilde{K}_a$ and the polytrophic law exponent m. Indeed some minor differences in these parameters, in respect to values obtained in [9], can be found, because they were tuned on a OWC/1 embodiment and without turbine.

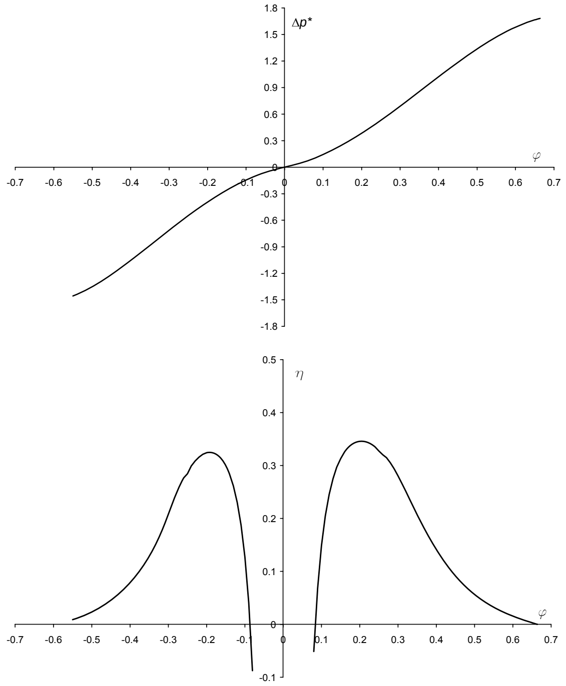

Fig. 4: Turbine pressure drop Δp^* and turbine efficiency η_t vs φ. The curves represent average values of 260 sea states recorded at sea on the small scale model of OWC/1 [5].

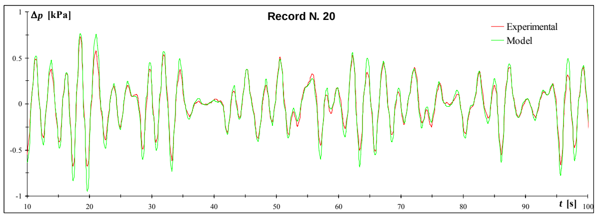

Fig. 5: Pressure fluctuations inside the central cell of the caisson. Red line: data recorded during a small scale field experiment [5]. Green line: numerical simulation with the linear model, using as an input values of the pressure fluctuations actually measured in the field.

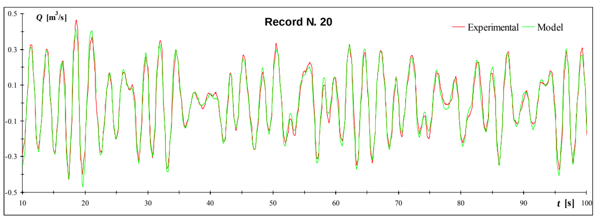

Fig. 6: Water discharge inside the central cell of the caisson. Red line: data recorded during a small scale field experiment [5]. Green line: numerical simulation with the linear model, using as an input values of the pressure fluctuations actually measured in the field.

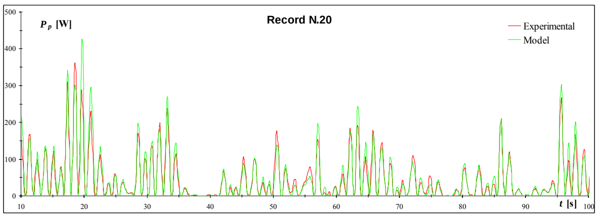

Fig. 7: Pneumatic power inside the central cell of the caisson. Red line: data recorded during a small scale field experiment [5]. Green line: numerical simulation with the linear model, using as an input values of the pressure fluctuations actually measured in the field.

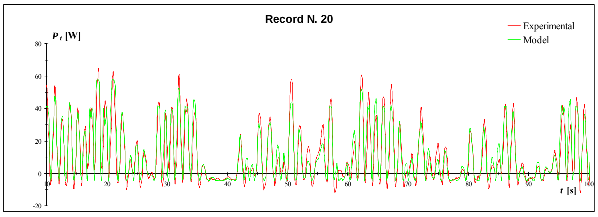

Fig. 8: Internal turbine power for one caisson (formed by three cells). Red line: data recorded during a small scale field experiment [5]. Green line: numerical simulation with the linear model, using as an input values of the pressure fluctuations actually measured in the field.

Tab. 1: working parameters of OWC. Comparison between measured and numerical data, time averaged during a sea state.

Record N. 20

Δp_{rms} [kPa]		Q_{rms} [m^3/s]		$\overline{P_p}$ [W]		$\overline{P_t}$ [W]	
Exp.	Num.	Exp.	Num.	Exp.	Num.	Exp.	Num.
312.6	409.1	0.062	0.068	57.0	69.8	12.0	14.6

Similar results have been obtained for all the 261 sea states recorded during the experimental campaign. Tab. 2 shows a general view of comparisons. Each value represents the average of its class. As an example, the value 0.0495 m^3/s of Q_{rms} (first row, fourth column) is the average of the Q_{rms} in the 73 records of the first class of data (i.e wind waves). And the value 0.0464 m^3/s (first row, fifth column) is the average of 73 records simulated numerically, using as an input the time history of the pressure fluctuations measured in the 73 records. We can see a systematic confirmation of the data relevant to a single record shown in tab. 1. Moreover we can see that predicted data are more accurate for swells. This is probably due to the better tuning of such waves with the plant. In fact the 95 records of swells have T_p = 4 s in average, that is a value very close to the eigenperiod of the plant.

4.2 "Stochastic behaviors" of the plant

The estimation of the turbine power output with the linearized model (Eq. 33) is based on the hypothesis that the non-dimensional flow coefficient φ be Gaussian in the time. Figs. 9 and 10 show the probability density function of φ values measured during record 100 and 117, respectively. Each record contains 3000 samples. The turbine speed was 1600 rpm during record 100 and 1800 rpm during record 117. For comparison, the figures indicate also the Gaussian probability density function.

The agreement is rather good, even if both distributions exhibit a minor discrepancy from the theoretical pdf for $0.3 < \varphi/\varphi_{rms} < 0.35$. This behaviour is probably due to the asymmetry of the water duct geometry, that in the reversing flow causes different values of minor losses according as the flow enters the plant or exits from it (see the cross section of Figs. 1 and 2).

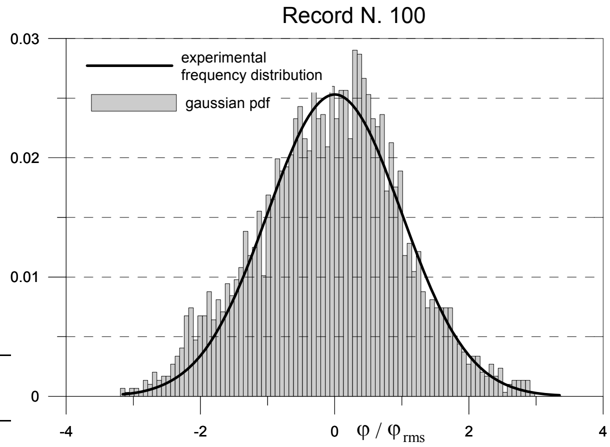

Fig. 9: Experimental frequency distribution during record 100. (Gaussian distribution is provided as reference).

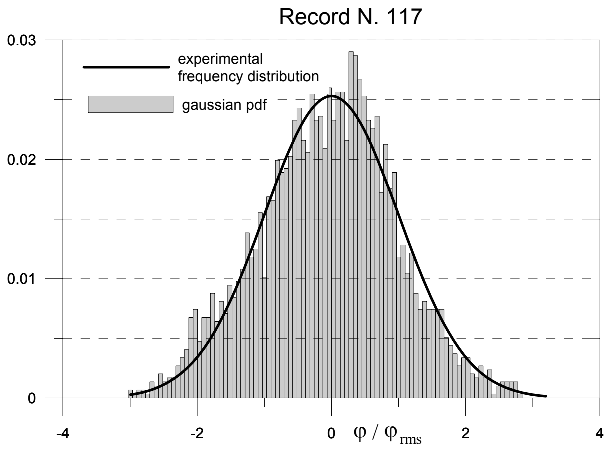

Fig. 10: Experimental frequency distribution during record 117. (Gaussian distribution is provided as reference).

Figs. 11-13 show the relationship between turbine mean efficiency $\overline{\eta}_t \equiv \overline{P}_t / \overline{P}_p$, Q_{rms} and Δp_{rms}, vs φ_{rms}, respectively. Red squares are experimental values of above listed variables, each one averaged along the record duration time. Green squares are the same averaged variables, simulated running the linear model in the time domain, using as an input the time history of the pressure fluctuation actually measured in the considered record. Moreover, in order to simulate the turbine presence, we adopted curves of Fig. 4.

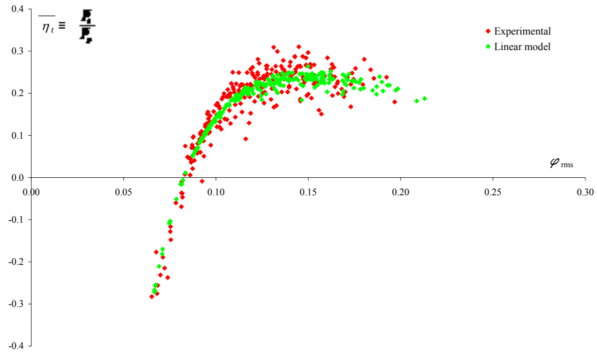

Fig. 11: $\overline{\eta}_t \equiv \overline{P}_t / \overline{P}_p$ vs φ_{rms}. Red squares: experimental data. Green squares: simulated data with the linearized model.

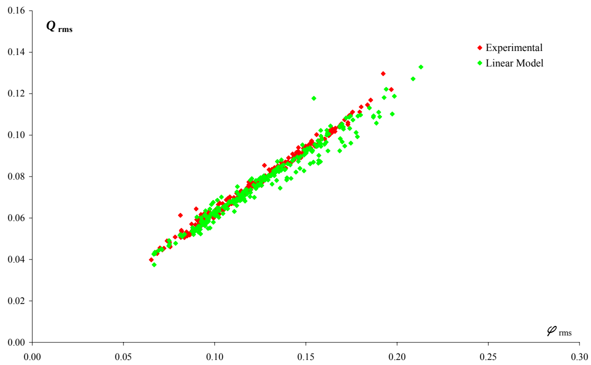

Fig. 12: Q_{rms} vs φ_{rms}.Red squares: experimental data. Green squares: simulated data with the linearized model.

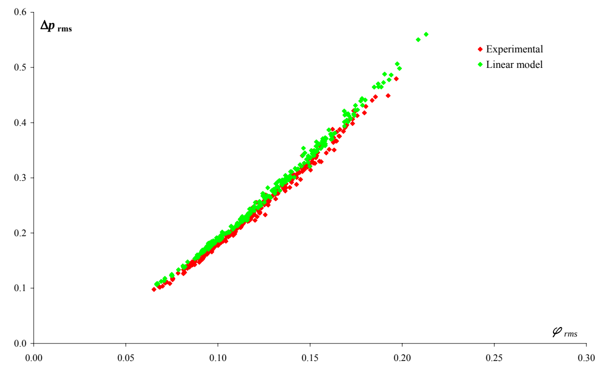

Fig. 13: Δp_{rms} vs φ_{rms}.Red squares: experimental data. Green squares: simulated data with the linearized model.

In details, Fig. 11 shows the average turbine efficiency (i.e. the ratio between the mean internal power transferred from air flow to the turbine and the pneumatic power). Experimental data are affected by a certain spread, quite justified considering the short duration of records (300 s). It is evident that green squares well interpret the mean trend of experimental values. This is a crucial result for the success of the stochastic model, whose principal target is to predict accurately and easily the power produced by the plant (see Eq. 34). Moreover, Figs. 12 and 13, show that the capability of stochastic model goes beyond the prediction of mean power. In fact, they asses the model is powerful also to predict the dynamic behaviors of the plant.

Class (°) (N. of records) / Data type	Δp_{rms} [kPa]		Q_{rms} [m^3/s]		P_p [W]		P_t [W]		φ_{rms}	
	Exp	Num	Exp	Num	Exp	Num	Exp	Num	Exp	Num
W (73)	274.9	307.8	0.0495	0.0464	33.0	39.9	9.16	12.59	0.115	0.104
W+S (61)	250.2	333.6	0.0501	0.0472	37.2	44.0	9.63	14.60	0.111	0.101
S (95)	355.7	443.9	0.0651	0.0654	64.9	73.2	20.02	21.57	0.136	0.124
LS (32)	355.8	434.6	0.0638	0.0602	61.9	71.5	20.33	21.31	0.129	0.116

Tab. 2 : values of OWC running parameters averaged for class of waves. Exp: measured data. Num: calculated data(°) Class 1: wind waves. Class 2: wind waves superimposed on swells. Class 3: swells. Class 4: long swells.

5 Conclusions

A stochastic approach has been presented to evaluate the average performance of a breakwater-converter embodying a new kind of OWC device (called REWEC), provided with an additional vertical duct at the wave-beaten side. The proposed methodology is based on two main assumptions:

(*a*) pressure fluctuations at the outer opening of the vertical duct can be mathematically represented by a Gaussian process of the time in the Stokes' expansion to the first order, whose one-dimensional power spectra is known;

(*b*) the relation between the dimensionless pressure drop across the Wells turbine and the flow coefficient is linear.

Unlike traditional OWCs, energy losses in the water flow cannot be neglected due to high velocities of water in the vertical duct. The dissipation effects have been taken into account by means of an adequacy coefficient which equates the energy dissipated in the actual turbulent flow (both in the vertical duct and in the air tube), time averaged during a sea state, to the average energy dissipated in a viscous flow.

Moreover, it has been shown that the linearized mathematical model is formally analogous to the mathematical model which describes the motion of a mechanical system constituted by masses, springs, and viscous dampers.

The results show a very good agreement with the model an experimental results. In particular we find that

(i) the model well predict the dynamic behaviors of the plant, provided that the characteristic curves of the turbine are well defined;

(ii) the analysis of distribution of φ_{rms} shows that it follows reasonably well the Gaussian pdf, apart for a circumscribed deviation, probably due to the asymmetry of the water duct geometry;

(iii) basic principles (*a*)-(*b*) of stochastic method are well supported by experimental evidences.

These results encourage to complement the formulation presented here for the analysis and optimal design (especially at the level of basic studies) of Wells-turbine-equipped REWEC plants. This aim can be achieved combining the stochastic approach with dimensional analysis, by characterizing both turbine geometry and economic aspects, and the wave climate for the considered location.

Acknowledgements

The careful work carried out by the graduated student Miss Graziella Carlo MSc is very appreciated.

References

[1] Lee CH, Newman JN, Nielsen FG. *Wave interactions with an oscillating water column.* Proceedings of the Sixth International Offshore and Polar Engineering Conference, Los Angeles, 1996. p. 82–90.

[2] Brito-Melo A, Hofmann T, Sarmento AJNA, Clèment AH, Delhommeau G. *Numerical modelling of OWC-shoreline devices including the effect of surrounding coastline and non-flat bottom.* Int J Offshore Polar Engng 2001; \11:147–54.

[3] Falcão A. F. de O., Justino P. A. P. *OWC wave energy devices with air flow control*. Ocean Engng 1999; 26:1275–95.

[4] Falcão A.F. de O., Rodrigues R.J.A., *Stochastic modelling of OWC wave power plant performance.* Applied Ocean Research 24, 2002; 59–71.

[5] Boccotti P., *Caisson breakwaters embodying an OWC with a small opening—Part I: Theory*. Ocean Engineering34, 2007 806-819.

[6] Boccotti P., Filianoti P., Fiamma V., Arena F., *Caisson breakwaters embodying an OWC with a small opening—Part II: A small-scale field experiment,* Ocean Engineering 34, 2007 820-841.

[7] Filianoti P., Camporeale S.M. (2005). *A linearized model for estimating the performance of sea wave energy converters (REWEC)*, Proceeding of the 6th European Wave and Tidal Energy Conference - Glasgow, UK. 29th august- 2nd september 2005,vol. 1, pp. 125-132

[8] Boccotti P., *Wave Mechanics for Ocean Engineering* . Elsevier Amsterdam, 1-495.